Thermodynamic Micellization Model for Asphaltene Precipitation Inhibition

Huanquan Pan and Abbas Firoozabadi
Reservoir Engineering Research Institute, Palto Alto, CA 94306

Aromatic solvents and oil-soluble amphiphiles are recognized as asphaltene precipitation inhibitors in oil production and transportation. In the absence of the model describing the effect of these inhibitors on asphaltene precipitation from crudes, proposed is a thermodynamic micellization model explaining the inhibition mechanism for both aromatic solvents and oil-soluble amphiphiles. The model shows that aromatic solvents are concentrated in the micellar shell, and the interfacial tension between the asphaltene micellar core and shell is reduced as the micelles becomes stabler. A crude, mixed with a small amount of an oil-soluble amphiphile, achieves a high micellar stability. The amphiphiles behave like resin species of the crude and coadsorb onto the micellar core with resins. The adsorption enthalpy of an amphiphile onto the micellar core is much higher than that of the resin and, therefore, amphiphiles can be very effective inhibitors. The results suggest that the adsorption enthalpy data can be used to screen the amphiphiles for asphaltene precipitation inhibition. For a given oil-soluble amphiphile, this model can predict the amount of the amphiphile required to inhibit the precipitation.

Introduction

An asphaltene species is defined as the heavy fraction of the crude, which is insoluble in normal heptane, but soluble in an aromatic solvent. This definition implies that an aromatic solvent can be a good solvent for asphaltene species; mixing aromatic solvents with crude can enhance the dissolution of asphaltene species. Some aromatic solvents have been used to inhibit the asphaltene precipitation in crudes (Cimino et al., 1995).

The Hildebrand solubility parameter (δ) has been used to describe the solvent power for dissolving asphaltene species (Speight, 1980; Lian et al., 1994). The solubility parameter of asphaltene, heptane, cyclohexane, and toluene are 9.50, 7.5, 8.2 and 8.9 $(\mathrm{cal/cm^3})^{0.5}$, respectively (Speight, 1980). The solubility parameter of an aromatic solvent is close to that of the asphaltene, and, therefore, it can fully dissolve the asphaltene species. A cycloparaffin with the same carbon number as a normal alkane can dissolve more asphaltene species, because the difference between asphaltene and a cycloparaffin solubility parameter is less than that between the asphaltene and the normal alkane. Hirshberg et al. (1984) used the Flory-Huggins theory to calculate the asphaltene solubility in a crude; the key parameter in their model is the asphaltene solubility parameter. De Boer et al. (1995) used the model of Hirshberg et al. to qualitatively screen crude oils for asphalt precipitation. The Flory-Huggins model, however, does not differentiate between asphaltene monomers and micelles.

Asphaltenes in aromatic solvent, crude, and aromatic/alkane mixtures form micelles (Sheu and Storm, 1995; Andersen and Speight, 1993; Rogacheva et al., 1980). Rogacheva et al. (1980) reported the critical micellar concentration (CMC) data of asphaltenes in toluene at different temperatures. In previous studies, Pan and Firoozabadi (1998, 2000) have developed a thermodynamic micellization model for crudes. In this model, resin molecules adsorb onto the surface of the asphaltene core. The resins stabilize the micelles. Chemicals, which have similar features as resins, are believed to help the asphaltene precipitation inhibition. However, a large concentration of resin and resin-like chemicals may be required for micellar stability as shown by Pan and Firoozabadi (1998, 2000), and will be shown in this study. The effect of an aromatic solvent on asphaltene stability in a crude has not been studied yet by a micellization model.

Correspondence concerning this article should be addressed to A. Firoozabadi.

Some chemicals such as oil-soluble amphiphiles (that is, surfactants) have been found to have a stronger effect on asphaltene precipitation inhibition than aromatic solvents. An amphiphile molecule has at least one polar head and a long-chain hydrocarbon tail, which is nonpolar. Gonzalez and Middea (1991) have investigated various oil-soluble amphiphiles including alkylbenzene, alkylalcohol, alkylamine and alkylphenol. They found that the polarity of the polar head plays a crucial role in stabilizing the asphaltene; p-alkylphenol was found to be an effective chemical. Chang and Fogler (1994a,b) studied the effect of alkylphenols, hydroxyethoxyalkylbenzene, and alkalbenzenesulfonic acids on the asphaltene stability in heptane/toluene mixtures. They found that the interaction between asphaltene and the polar head of an amphiphile is an important parameter in stabilizing the asphaltene in solution. Alkalbenzenesulfonic acid is more effective than alkylphenols, which, in turn, are more effective than hydroxyethoxyalkylbenzene. The strong interaction between the asphaltene and the HSO_3 group of alkalbenzenesulfonic acid was studied by infrared spectroscopy and small-angle X-ray scattering. De Boer et al. (1995) found that the C_{18}-sulphonic acid is more effective than salicylic acid, even though they have the same chain length. These investigators also observed that an amphiphile should be an acid or acid-like; since only the H^+ proton interacts with the asphaltene, if the H^+ is replaced by another group, the amphiphile may lose its activity (De Boer et al., 1995). The amphiphiles with a strong acid group are very effective, but an amphiphile with multiple strong acid groups, such as C_{16}-alkyl diphenyl-oxide di-sulfonic acid (De Boer et al., 1995), tends to self-associate due to the fact that the interaction between the amphiphile molecules is stronger than the interaction between the asphaltene and amphiphile molecules. This strong interaction increases the asphaltene stability significantly, reducing the concentration of the inhibitor, thus economizing the asphaltene precipitation inhibition. However, the amphiphiles, which have a strong acid group, may self-associate and precipitate in the crude beyond a certain concentration. This behavior has been observed by Chang and Fogler (1994a) for p-(n-dodecyl)benzenesulfonic acid. Therefore, an optimal concentration may exist for practical applications.

Asphaltene precipitation from crudes has been modeled by Pan and Firoozabadi (1998, 2000) using thermodynamics of micellization, where the micellar shell is assumed to contain only the resin and deasphalt oil. The resin is assumed to adsorb onto the micellar core. The deasphalt oil which contains all crude components except asphaltene and resin species is assumed to have the same composition in the shell as in the bulk phase. The above model is used to predict the precipitation due to pressure, temperature, and composition changes. The predictions are in good agreement with data (Pan and Firoozabadi, 2000). Asphaltene precipitation was recently predicted during both the depletion of 12 reservoir crudes and the mixing of H_2S with one crude (Iyer, 1998). The predicted results are in good agreement with measurements, confirming further the prediction capability of our micellar model. The predicted results also show that the Gibbs free energy of association of an asphaltene molecule (Eq. 5) is an important parameter of the micellization model. The Gibbs free energy of association of an asphaltene molecule is a measure of polarity of asphaltene species.

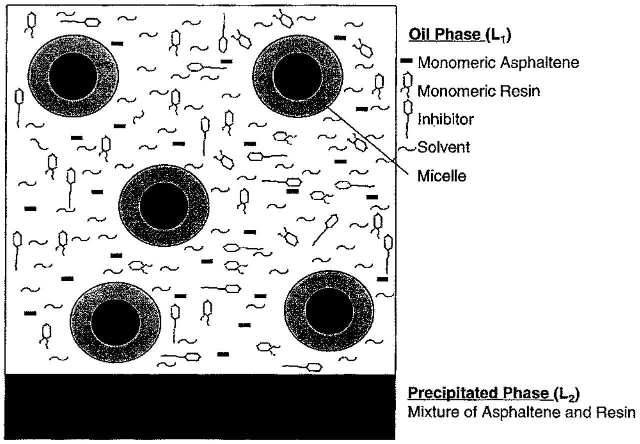

Figure 1. Crude inhibitor system.

The major objective of this work is the study of asphaltene precipitation inhibition from crudes using a thermodynamic micellization model. Two different inhibitors are considered: (1) aromatic solvents; (2) amphiphiles. No attempt has yet been made in the literature to model the effect of amphiphiles on asphaltene precipitation inhibition. In fact, most of the models including the equation-of-state approach and the solubility parameter approach may not have the flexibility to describe the phase behavior of crude/amphiphile mixtures. Using our micellization model for the description of asphaltene precipitation inhibition requires modification to account for the adsorption of amphiphiles onto the micellar core and the partitioning of the aromatic solvent in the shell and the bulk phase. Figure 1 shows the crude/inhibitor system. The precipitated phase is a liquid mixture of asphaltene and resin at high temperatures. The inhibitor is either an aromatic solvent (with a small tail or without a tail) or an amphiphile (with a long tail). In the following, the model for the crude/aromatic solvent is first presented followed by the model for the crude/amphiphile.

Modeling of Asphaltene Precipitation Inhibition

Crude/aromatic solvent system

Based on experimental data, Wiehe and Liang (1996) suggest that the asphaltene molecules aggregate to form the micellar core in crudes; the core is surrounded by resins and a high concentration of aromatic species. We should point out that the aggregation of asphaltene molecules is different in crude oil/water and in crude oil systems. In a crude oil/water system, the asphaltene molecules behave like a surfactant and adsorb onto the surface of water droplets to form water-in-oil emulsions. However, one cannot divide an asphaltene molecule into a polar head and a nonpolar tail as surfactants such as amphiphiles do. In a crude oil, asphaltene molecules do not act as a surfactant, but resin molecules do. In our micellization model, we integrate the suggestion of Wiehe and Liang (1996) and propose the micellar structure shown in Figure 2. Note that the concentration of aromatic solvent is different in the micellar shell and in the bulk liquid (phase L_1 in Figure 1). For simplicity, we assign all species of the

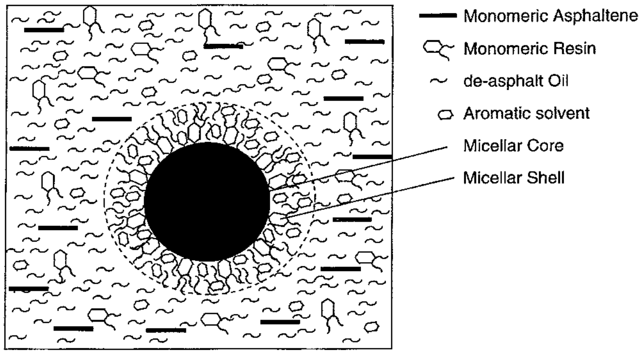

Figure 2. Micelle in mixture of crude/aromatic solvent.

deasphalt crude as a single pseudocomponent for the purpose of equilibrium between the shell and the bulk phase.

The Gibbs free energy G for the crude/aromatic mixture can be expressed as

$$\begin{aligned} G = {} & \sum_{i=1}^{Nc} N_i \mu_i^0(T) + N_m \Delta G_m^{00} \\ & + kT\left(\sum_{i=1}^{Nc-3} N_i^{L_1} \ln x_i + N_m \sum_{i=1}^{Nc-3} n_i^{sh} \ln x_i^{sh} \right) \\ & + kT\left(N_s^{L_1} \ln x_s + N_m n_s^{sh} \ln x_s^{sh} \right) \\ & + kT\left(N_{a_1} \ln x_{a_1} + N_{r_1} \ln x_{r_1} + N_m \ln x_m \right) \\ & + kT \sum_{i=1}^{Nc} N_i^{L_1} \ln \hat{\varphi}_i P \\ & + kT\left(N_a^{L_2} \ln \hat{f}_a^{L_2} + N_r^{L_2} \ln \hat{f}_r^{L_2} \right) \end{aligned} \quad (1)$$

In the above equation, Nc denotes the total number of species. The indices for aromatic, resin and asphaltene species are Nc-2, Nc-1, and Nc, respectively. The superscript 0, sh, L_1, and L_2 represent standard state, the micellar shell, the light bulk phase and the precipitated phase in that order (see Figure 1). The subscripts i, m, s, a_1, r_1, a and r represent the component index, micelle, aromatic solvent, asphaltene monomer, resin monomer, overall asphaltene and overall resin, respectively. In Eq. 1, the terms on the right hand side according to order are: the standard Gibbs free energy of all species in the monomeric state; the standard micellization energy; the mixing energy of solvent species in the shell and the bulk phase; the mixing energy of aromatic solvent in the shell and the bulk phase; the mixing energy of monomeric asphaltenes, monomeric resins and micelles; the interaction energy for all species using the mean-field approximation; and the Gibbs free energy from the precipitated phase, respectively. The detailed derivation of Eq. 1 is given by Pan and Firoozabadi (1998, 2000). The key parameter for the micellar stability in Eq. 1 is the standard Gibbs free energy of micellization ΔG_m^{00}, which is defined as

$$\Delta G_m^{00} = \mu_m^* - n_1 \mu_{a_1}^* - n_2 \mu_{r_1}^* \quad (2)$$

ΔG_m^{00} is a complicated function of micellar size and solvent composition in the shell and in the bulk phase. We have proposed a reversible micellar formation process for the evaluation of ΔG_m^{00} (Pan and Firoozabadi, 1998)

$$\begin{aligned} \Delta G_m^{00} = {} & \left[\left(\Delta G_a^0\right)_{\mathrm{Ass}} + \left(\Delta G_a^0\right)_{\mathrm{Tr}} + \left(\Delta G_a^0\right)_{\mathrm{Def}} \right] \\ & + \left[\left(\Delta G_r^0\right)_{\mathrm{Inf}} + \left(\Delta G_r^0\right)_{\mathrm{Adp}} + \left(\Delta G_r^0\right)_{\mathrm{Str}} + \left(\Delta G_r^0\right)_{\mathrm{Tr}} + \left(\Delta G_r^0\right)_{\mathrm{Def}} \right] \end{aligned} \quad (3)$$

In Eq. 3, the terms in the first square brackets are the association energy between the asphaltene molecules in the micellar core, the transfer energy of asphaltene molecules from the bulk phase to the core, and the deformation energy of the asphaltene molecules in the shell, respectively. The terms in the second brackets are a result of the interfacial energy of the asphaltene core and solvent in the shell, the adsorption energy of the resin onto the micellar core, the steric repulsion energy of resin in the shell, the transfer energy of resin molecules from the dilute bulk phase to the shell, and the deformation energy of resin molecules in the shell, respectively. An alternative form of Eq. 3 using one molecule of asphaltene and resin is

$$\begin{aligned} \Delta G_m^{00} = {} & n_1\left[\left(\Delta g_a^0\right)_{\mathrm{Ass}} + \left(\Delta g_a^0\right)_{\mathrm{Tr}} + \left(\Delta g_a^0\right)_{\mathrm{Def}} \right] \\ & + n_2\left[\left(\Delta g_r^0\right)_{\mathrm{Inf}} + \left(\Delta h_r^0\right)_{\mathrm{Adp}} + \left(\Delta g_r^0\right)_{\mathrm{Str}} + \left(\Delta g_r^0\right)_{\mathrm{Tr}} + \left(\Delta g_r^0\right)_{\mathrm{Def}} \right] \end{aligned} \quad (4)$$

After substitution of various terms in Eq. 4 (Pan and Firoozabadi, 1998), one obtains

$$\begin{aligned} & \Delta G_m^{00}/kT \\ & = n_1\left[\Delta g_a^0/kT + \ln\left(\varphi_a^l/\varphi_{a1}^\infty\right) + \frac{1}{2}\left(\frac{R^2}{m_a L^2} + 2\frac{m_a^{1/2} L}{R} - 3 \right) \right] \\ & \quad + n_2\left[\sigma(a - a_0)/kT + \left(\Delta h_r^0\right)_{\mathrm{Adp}}/kT - \ln\left(1 - \frac{a_p}{a}\right) \right. \\ & \quad \left. + \ln\left(\varphi_{r,s}^l x_{r,s}/\varphi_r^\infty\right) + \frac{1}{2}\left(\frac{D^2}{m_r L^2} + 2\frac{m_r^{1/2} L}{D} - 3 \right) \right], \end{aligned} \quad (5)$$

where

$$R = \left(\frac{3}{4\pi} n_1 v_\alpha \right)^{1/3} \quad (6)$$

$$m_a = v_a/v_l \quad (7a)$$

$$m_r = v_r/v_l \quad (7b)$$

$$L = v_l^{1/3} \quad (8)$$

$$a = 4\pi R^2/n_2. \quad (9)$$

In Eq. 5, n_1 and n_2 are the number of asphaltene and resin molecules in the micelle, and Δg_a^0 is the association free energy per asphaltene molecule in the micellar core. The symbols φ, R, L and D represent the fugacity coefficient, the micellar radius, the characteristic length of a molecule, and the shell thickness, respectively. The term $\sigma n_2(a - a_0)$ in Eq. 5 represents the interfacial Gibbs free energy of a micelle, and σ is the tension at the interface of the micellar core and the shell. This term is positive, and, therefore, opposes the micellar formation. The interfacial tension σ can be evaluated from (Pan and Firoozabadi, 2000)

$$\sigma = \frac{kT}{L^2} \cdot \left(\frac{V_a(\delta_{sl} - \delta_a)^2}{6kT} \right)^{0.65} \tag{10}$$

where δ_{sl} and δ_a are solubility parameters of the deasphalt crude/aromatic solvent in the shell, and asphaltene in the core, respectively. The solubility parameter of the deasphalt crude/aromatic solvent mixture δ_{sl} is calculated from

$$\delta_{sl} = \Psi_l \delta_l + \Psi_s \delta_s \tag{11}$$

where Ψ is the volume fraction. The subscript l represents the deasphalt crude, δ_s is closer to δ_a than δ_l, and δ_{sl} becomes close to δ_a when the concentration of the aromatic solvent increases in the shell. Consequently, the interfacial tension σ and the interfacial free energy decrease, as the concentration of the aromatic species increases in the shell and the micelle becomes more stable. The high concentration of aromatic solvent in the micellar shell stabilizes the micelle in the crude.

There are 12 unknowns in Eq. 1: n_1, n_2, n_l^{sh}, n_s^{sh}, D, $N_l^{L_1}$, $N_s^{L_1}$, $N_{a_1}^{L_1}$, $N_{r_1}^{L_1}$, $N_m^{L_1}$, $N_a^{L_2}$, and $N_r^{L_2}$. The feasible sequential quadratic programming (FSQP) algorithm (Zhou et al., 1996) is used to minimize the Gibbs free energy given by Eq. 1 with respect to these variables. The minimization is subject to the following material balance constraints

$$N_a = N_{a_1}^{L_1} + n_1 N_m^{L_1} + N_a^{L_2} \tag{12a}$$

$$N_r = N_{r_1}^{L_1} + n_2 N_m^{L_1} + N_r^{L_2} \tag{12b}$$

$$N_l = N_l^{L_1} + n_l^{sh} N_m^{L_1} \tag{12c}$$

$$N_s = N_s^{L_1} + n_s^{sh} N_m^{L_1} \tag{12d}$$

and the micellar shell volume constraint

$$\frac{4\pi}{3}\left[(R + D)^3 - R^3 \right] = (n_2 + n_l + n_s) v^{sh}. \tag{12e}$$

In Eq. 12e, v^{sh} is the molecular volume of the mixture in the shell, and the lefthand side of Eq. 12e is the total shell volume surrounding a micellar core. The value of these 12 variables at the global minimum of Gibbs free energy provides the micellar size, the aromatic solvent composition in the shell, the amount of monomeric asphaltene, monomeric resin, micelle, aromatic solvent in the bulk phase, and the amount of asphaltene and resin in the precipitated phase.

We select first a mixture of the Weyburn reservoir crude and CO_2 (Sirvastava et al., 1995) to examine the effect of aromatic solvents on precipitation inhibition. The detailed characterization of this reservoir fluid is described by Pan and Firoozabadi (2000), and the composition is listed in Table 1. Three aromatic solvents, benzene, toluene, and o-xylene, are examined in this study. Figure 3 shows the amount of precipitated asphaltene vs. mole fraction of CO_2 in the crude/CO_2/benzene mixture for different benzene concentrations. An increase in benzene concentration decreases the amount of precipitation. Figure 3 also shows that the onset concentration of CO_2 increases faster at low benzene concentrations than it does at high concentrations. These results are in agreement with experimental observations by Cimino et al. (1995). Similar results are shown in Figures 4 and 5 with toluene and o-xylene. Figure 6 plots the amount of precipitated asphaltene vs. the mole fraction of CO_2 in the crude/CO_2/aromatic mixture with 1% of the three aromatic solvents. O-xylene has the most effectiveness, and toluene is somewhat more effective than benzene. Figure 7 shows the

Table 1. Composition of Weyburn Reservoir Fluid

Component	mol %	M (g/mol)
N_2	0.96	
CO_2	0.58	
H_2S	0.30	
C_1	4.49	
C_2	2.99	
C_3	4.75	
i-C_4	0.81	
n-C_4	1.92	
i-C_5	1.27	
n-C_5	2.19	
$C_{6\text{-}9}$	25.73	105
$C_{10\text{-}17}$	26.98	179
$C_{18\text{-}27}$	13.28	312
C_{28+}	13.75	576*
CP1	6.69	442
CP2	4.359	582
r	1.839	850
a	0.862	1000

*Estimated from TBP data.
wt. % of asphaltene and resin is 4.9 and 8.9, respectively in tank oil.

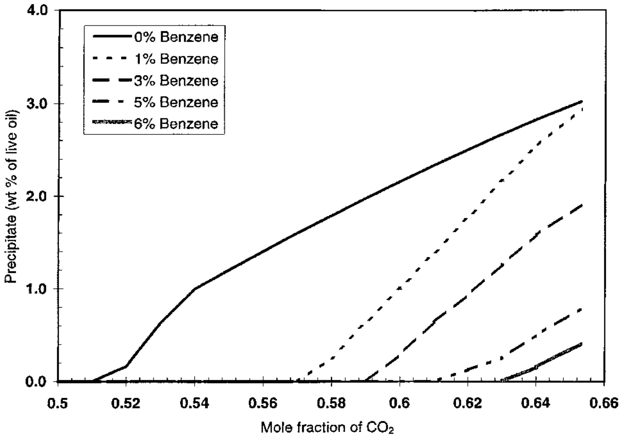

Figure 3. Effect of benzene concentration (mol %) on asphaltene precipitation.

Weyburn reservoir fluid and CO_2 mixture at 160 bar and 332 K.

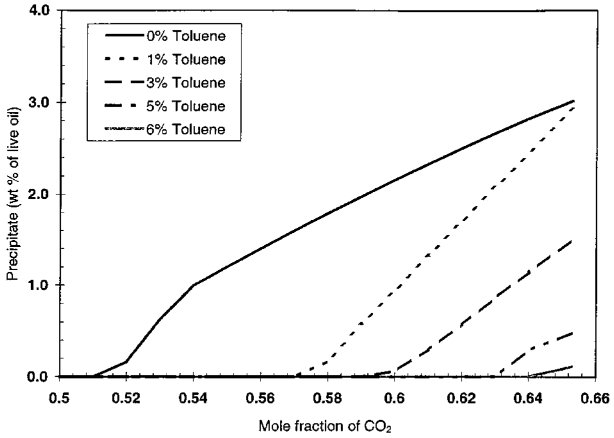

Figure 4. Effect of toluene concentration (mol %) on alphaltene precipitation.

Weyburn reservoir fluid and CO_2 mixture at 160 bar and 332 K.

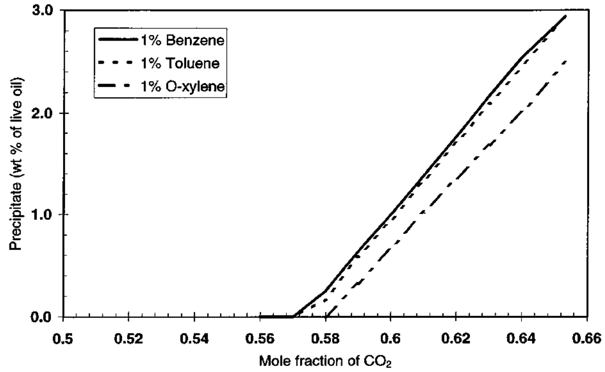

Figure 6. Effect of aromatic on asphaltene precipitation.

Weyburn reservoir fluid and CO_2 mixture at 160 bar and 332 K.

same pattern for the crude with 3% of aromatic solvents. Experimental observations have revealed that when an aromatic solvent is mixed with a crude, the micellar size decreases (Espinat and Ravey, 1993). Figure 8 also shows that the model predicts a decrease in the micellar size upon mixing the aromatic solvent with the crude. Figure 9 plots the predicted concentration ratio of the aromatic solvent in the shell to the bulk phase; the ratio is about 3.0 at low CO_2 concentrations. At first, an increased CO_2 concentration will cause the ratio to increase slowly but when CO_2 concentration approaches the precipitation point, the ratio increases quickly. The figure also shows that the sequence of the ratio values is o-xylene > toluene > benzene for given CO_2 and aromatic concentrations. Figure 10 plots ratio of the toluene in the shell to the bulk phase for two different concentrations. The difference is very small, especially at high CO_2 concentrations. The high efficiency of o-xylene among the three aromatic solvents can be explained. First, o-xylene has the highest ratio of the concentration between the shell and bulk; secondly, its molar volume is the largest. Since the solubility parameter of the solvent mixture is proportional to the volume fraction of aromatic, o-xylene provides a larger volume fraction than the other two aromatic solvents at the same mole fraction. Figure 11 plots the interfacial tension between the micellar core and the shell vs. CO_2 mole fraction at different toluene concentrations. The interfacial tension increases with the increase of the CO_2 concentration. Mixing toluene with crude decreases the interfacial tension. Note that the interfacial tension values are high at high CO_2 concentrations, which may be a reflection of the inadequacy of the σ model used in this work.

Next, the thermodynamic micellization model for a crude/oil-soluble amphiphile mixture is presented.

Crude/Oil-soluble amphiphile system

The thermodynamic micellization model (Pan and Firoozabadi, 1998, 2000; Firoozabadi, 1999) is modified to allow for the co-adsorption of amphiphile species similar to resin species. Amphiphile molecules in the shell reversibly equilibrate with amphiphile monomers in the bulk phase. The crude/amphiphile mixture is a mixed surfactant (resin and amphiphile) system. Figure 12 sketches a micelle of a

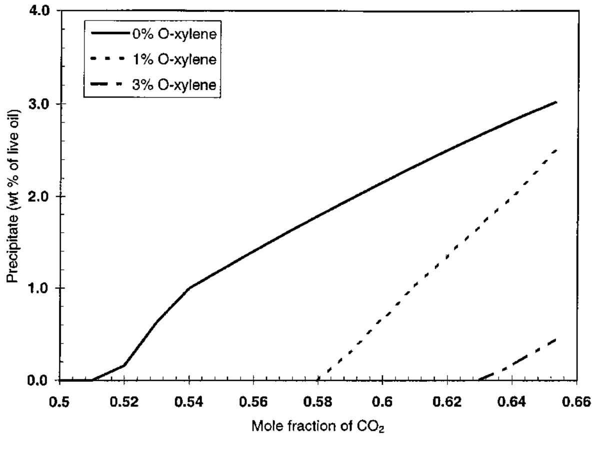

Figure 5. Effect of o-xylene concentration (mol %) on alphaltene precipitation.

Weyburn reservoir fluid and CO_2 mixture at 160 bar and 332 K.

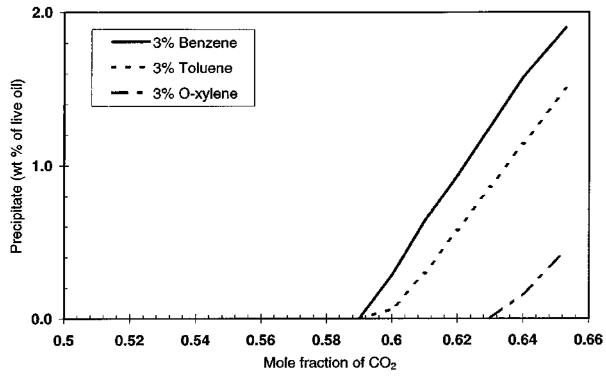

Figure 7. Effect of aromatic on asphaltene precipitation.

Weyburn reservoir fluid and CO_2 mixture at 160 bar and 332 K.

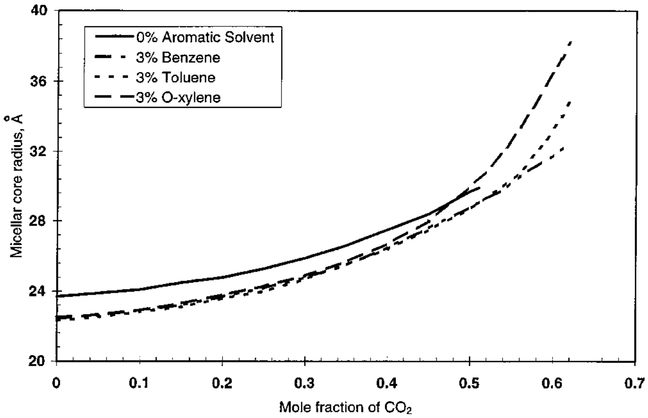

Figure 8. Effect of different aromatics on micellar size.

Weyburn reservoir fluid and CO$_2$ mixture at 160 bar and 332 K.

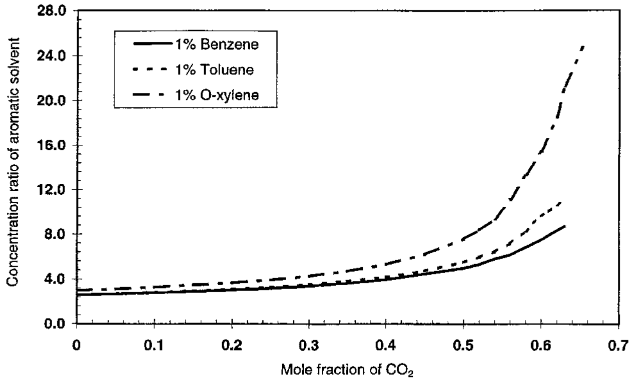

Figure 9. Concentration ratio of aromatic solvent in the micellar shell and bulk phase.

Weyburn reservoir fluid and CO$_2$ mixture at 160 bar and 332 K.

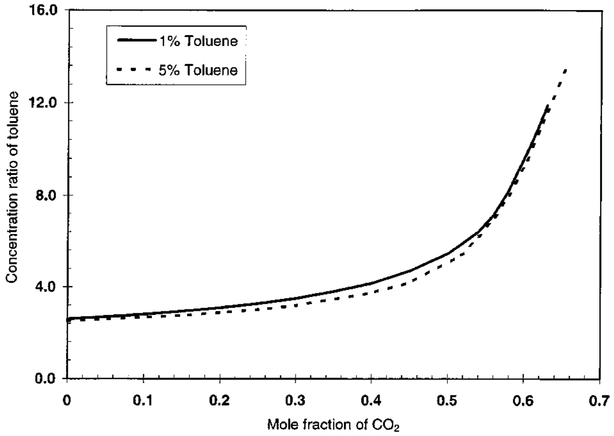

Figure 10. Concentration ratio of toluene between micellar shell and bulk phase.

Weyburn reservoir fluid and CO$_2$ mixture at 160 bar and 332 K.

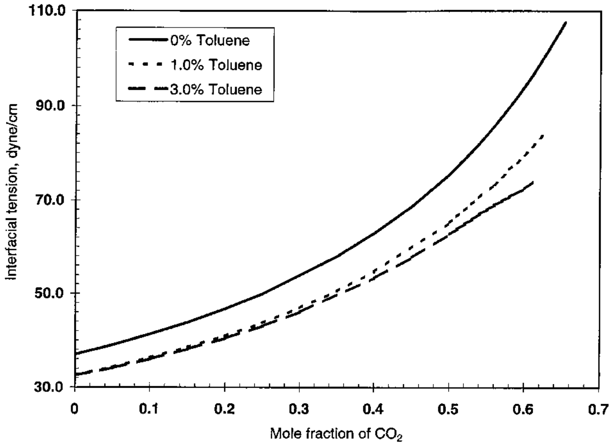

Figure 11. Interfacial tension between the micellar core and the shell at different toluene concentrations.

Weyburn reservoir fluid and CO$_2$ mixture at 160 bar and 332 K.

crude/amphiphile mixture. In the following expressions, component indices for asphaltene, resin, and amphiphile species are Nc, $Nc-1$, and $Nc-2$, respectively. The Gibbs free energy of a two-phase crude/amphiphile-precipitated system (see Figure 1) can be expressed by

$$\begin{aligned} G = {} & \sum_{i=1}^{Nc} N_i \mu_i^0(T) + N_m \Delta G_m^{00} \\ & + kT\left(\sum_{i=1}^{Nc-3} N_i^{L_1} \ln x_i + \sum_{i=1}^{Nc-3} n_i^{sh} \ln x_i^{sh} \right) \\ & + kT\left(N_{f_1} \ln x_{f_1} + N_{r_1} \ln x_{r_1} + N_{a_1} \ln x_{a_1} + N_m \ln x_m \right) \\ & + kT \sum_{i=1}^{Nc} N_i \ln \hat{\varphi}_i P + kT\left(N_a^{L_2} \ln \hat{f}_a^{L_2} + N_r^{L_2} \ln \hat{f}_r^{L_2} \right), \end{aligned} \tag{13}$$

where the subscript f denotes the amphiphile species. In Eq. 13, the standard Gibbs free energy of micellization ΔG_m^{00} can be expressed as

$$\Delta G_m^{00} = \mu_m^* - n_1 \mu_{a_1}^* - n_2 \mu_{r_1}^* - n_f \mu_{f_1}^*, \tag{14}$$

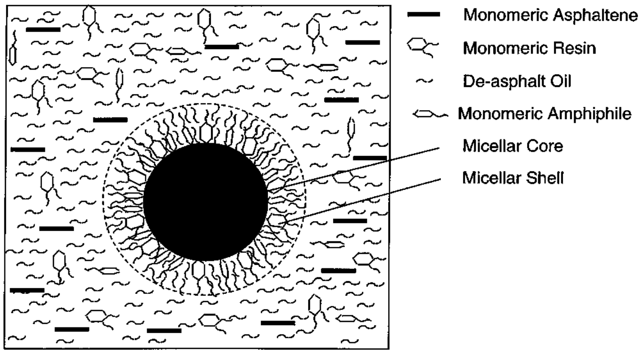

Figure 12. Micelle in the crude/amphiphile mixture.

where n_f is the molecular number of the amphiphile in the shell, and $\mu_{f_1}^*$ is the chemical potential of the monomeric amphiphile molecule at infinite dilution of deasphalt crude. An expression similar to Eq. 3 can be written for ΔG_m^{00}

$$\begin{aligned}\Delta G_m^{00} = & \left[\left(\Delta G_a^0\right)_{\mathrm{Ass}} + \left(\Delta G_a^0\right)_{\mathrm{Tr}} + \left(\Delta G_a^0\right)_{\mathrm{Def}}\right] \\ & + \left[\left(\Delta G_r^0\right)_{\mathrm{Adp}} + \left(\Delta G_r^0\right)_{\mathrm{Tr}} + \left(\Delta G_r^0\right)_{\mathrm{Def}}\right] \\ & + \left[\left(\Delta G_f^0\right)_{\mathrm{Adp}} + \left(\Delta G_f^0\right)_{\mathrm{Tr}} + \left(\Delta G_f^0\right)_{\mathrm{Def}}\right] \\ & + (\Delta G^0)_{\mathrm{Inf}} + (\Delta G^0)_{\mathrm{Ste}} \end{aligned} \tag{15}$$

Note that the terms in the third bracket represent the contribution of the amphiphile species to the standard Gibbs free energy of micellization. The interfacial and steric repulsion energies (the last two terms on the righthand side of Eq. 15) for the mixed surfactant system differ from the single surfactant system. The expression of $(\Delta G^0)_{\mathrm{Inf}}$ is given by

$$\begin{aligned}(\Delta G^0)_{Inf} & = \sigma\left[(n_2 + n_f)a - n_2 a_{0,r} - n_f a_{0,f}\right] \\ & = \sigma\left[n_2(a - a_{0,r}) + n_f(a - a_{0,f})\right]\end{aligned} \tag{16}$$

where

$$a = 4\pi R^2/(n_2 + n_f) \tag{17}$$

and R is given by Eq. 6. The $(\Delta G^0)_{\mathrm{Inf}}$ can be divided into the contributions due to the resin and amphiphile species

$$(\Delta G^0)_{Inf} = \left(\Delta G_r^0\right)_{Inf} + \left(\Delta G_f^0\right)_{Inf} \tag{18}$$

and

$$\left(\Delta G_r^0\right)_{Inf} = n_2\left(\Delta g_r^0\right)_{Inf} = n_2\sigma(a - a_{0,r}) \tag{19a}$$

$$\left(\Delta G_f^0\right)_{Inf} = n_f\left(\Delta g_f^0\right)_{Inf} = n_f\sigma(a - a_{0,f}). \tag{19b}$$

The general expression for steric repulsion energy of the mixed surfactants is given by (Puvvada and Blankschtein, 1992; Nagarajan, 1986)

$$(\Delta G^0)_{\mathrm{Ste}} = -kT(n_2 + n_f)\ln\left(1 - \frac{n_2 a_{p,r} + n_f a_{p,f}}{(n_2 + n_f)a}\right) \tag{20}$$

If the amphiphile species has the same effective cross-sectional area a_p as resin, Eq. 20 simplifies to

$$(\Delta G^0)_{\mathrm{Ste}} = -kT\left[n_2 \ln\left(1 - \frac{a_{p,r}}{a}\right) + n_f \ln\left(1 - \frac{a_{p,f}}{a}\right)\right]. \tag{21}$$

If the cross-section areas a_p of the resin and amphiphile species are close to each other, Eq. 21 can be a good approximation to Eq. 20 (Puvvada and Blankschtein, 1992). We examined the $(\Delta G^0)_{\mathrm{Ste}}$ using Eqs. 20 and 21; the two expressions give almost the same result. However, the computations using Eq. 21 are much more stable than they are using Eq. 20. In our computations, we use Eq. 21 to calculate $(\Delta G^0)_{\mathrm{Ste}}$ and divide it into two parts

$$(\Delta G^0)_{\mathrm{Ste}} = \left(\Delta G_r^0\right)_{\mathrm{Ste}} + \left(\Delta G_f^0\right)_{\mathrm{Ste}} \tag{22}$$

where

$$\left(\Delta G_r^0\right)_{\mathrm{Ste}} = n_2\left(\Delta g_r^0\right)_{\mathrm{Ste}} = -n_2 kT \ln\left(1 - \frac{a_{p,r}}{a}\right) \tag{23a}$$

$$\left(\Delta G_r^0\right)_{\mathrm{Ste}} = n_f\left(\Delta g_f^0\right)_{\mathrm{Ste}} = -n_f kT \ln\left(1 - \frac{a_{p,f}}{a}\right) \tag{23b}$$

Introducing Eqs. 22 and 18 into Eq. 15, ΔG_m^{00} can be rewritten in the symmetrical form

$$\begin{aligned}\Delta G_m^{00} = & \left[\left(\Delta G_a^0\right)_{\mathrm{Ass}} + \left(\Delta G_a^0\right)_{\mathrm{Tr}} + \left(\Delta G_a^0\right)_{\mathrm{Def}}\right] \\ & + \left[\left(\Delta G_r^0\right)_{\mathrm{Inf}} + \left(\Delta G_r^0\right)_{\mathrm{Ste}} + \left(\Delta G_r^0\right)_{\mathrm{Adp}} + \left(\Delta G_r^0\right)_{\mathrm{Tr}} + \left(\Delta G_r^0\right)_{\mathrm{Def}}\right] \\ & + \left[\left(\Delta G_f^0\right)_{\mathrm{Inf}} + \left(\Delta G_f^0\right)_{\mathrm{Ste}} + \left(\Delta G_f^0\right)_{\mathrm{Adp}} + \left(\Delta G_f^0\right)_{\mathrm{Tr}} + \left(\Delta G_f^0\right)_{\mathrm{Def}}\right]. \end{aligned} \tag{24}$$

The advantage of Eq. 24 is the simplicity for its extension to a multisurfactant system. Equation 24 can be rewritten as follows using Gibbs free energy per molecule

$$\begin{aligned}\Delta G_m^{00} + n_1 & \left[\left(\Delta g_a^0\right)_{\mathrm{Ass}} + \left(\Delta g_a^0\right)_{\mathrm{Tr}} + \left(\Delta g_a^0\right)_{\mathrm{Def}}\right] \\ & + n_2\left[\left(\Delta g_r^0\right)_{\mathrm{Inf}} + \left(\Delta g_r^0\right)_{\mathrm{Ste}} + \left(\Delta h_r^0\right)_{\mathrm{Adp}} + \left(\Delta g_r^0\right)_{\mathrm{Tr}} + \left(\Delta g_r^0\right)_{\mathrm{Def}}\right] \\ & + n_f\left[\left(\Delta g_f^0\right)_{\mathrm{Inf}} + \left(\Delta g_f^0\right)_{\mathrm{Ste}} + \left(\Delta h_f^0\right)_{\mathrm{Adp}} + \left(\Delta g_f^0\right)_{\mathrm{Tr}} + \left(\Delta g_f^0\right)_{\mathrm{Def}}\right]. \end{aligned} \tag{25}$$

After substitution of various terms in Eq. 25,

$$\begin{aligned} & \Delta G_m^{00}/kT \\ & = n_1\left[\Delta g_a^0/kT + \ln\left(\varphi_a^l/\varphi_{a_1}^{\infty}\right) + \frac{1}{2}\left(\frac{R^2}{m_a L^2} + 2\frac{m_a^{1/2} L}{R} - 3\right)\right] \\ & \quad + n_2\left[\sigma(a - a_{0,r})/kT + \left(\Delta h_r^0\right)_{\mathrm{Adp}}/kT - \ln\left(1 - \frac{a_{p,r}}{a}\right)\right. \\ & \quad \left. + \ln\left(\varphi_{r,s}^l x_{r,s}/\varphi_r^{\infty}\right) + \frac{1}{2}\left(\frac{D^2}{m_r L^2} + 2\frac{m_r^{1/2} L}{D} - 3\right)\right] \\ & \quad + n_f\left[\sigma(a - a_{0,f})/kT + \left(\Delta h_f^0\right)_{\mathrm{Adp}}/kT - \ln\left(1 - \frac{a_{p,f}}{a}\right)\right. \\ & \quad \left. + \ln\left(\varphi_{f,s}^l x_{f,s}/\varphi_f^{\infty}\right) + \frac{1}{2}\left(\frac{D^2}{m_f L^2} + 2\frac{m_f^{1/2} L}{D} - 3\right)\right], \end{aligned} \tag{26}$$

where

$$m_f = \upsilon_f/\upsilon_l. \tag{27}$$

Substitution of ΔG_m^{00} from Eq. 26 into Eq. 13 results in 12 unknowns in Eq. 13: n_1, n_2, n_f, n_l^{sh}, D, $N_{a_1}^{L_1}$, $N_{r_1}^{L_1}$, $N_f^{L_1}$, $N_m^{L_1}$,

$N_l^{L_1}$, $N_a^{L_2}$, $N_r^{L_2}$. Similar to the previous case, the FSQP algorithm is used to minimize the Gibbs free energy with respect to these variables. The minimization is subject to the following material balance and the shell volume constraints

$$N_a = N_{a_1}^{L_1} + n_1 N_m^{L_1} + N_a^{L_2} \tag{28a}$$

$$N_r = N_{r_1}^{L_1} + n_2 N_m^{L_1} + N_r^{L_2} \tag{28b}$$

$$N_f = N_{f_1}^{L_1} + n_f N_m^{L_1} \tag{28c}$$

$$N_l = N_l^{L_1} + n_l^{sh} N_m^{L_1} \tag{28d}$$

$$\frac{4\pi}{3}\left[(R+D)^3 - R^3\right] = (n_2 + n_l + n_f)v^{sh}. \tag{28e}$$

The value of these 12 variables at the global minimum of Gibbs free energy provides the solution. In the following, the results for the crude/oil-soluble amphiphile systems are presented. Similar to the crude/aromatic solvent model, the Weyburn reservoir crude is used.

Resin is a natural surfactant for asphaltene stability in the crude. The effect of resin concentration on asphaltene precipitation inhibition is discussed. The results are discussed for the amphiphile p-(n-dodecyl)benzenesulfonic acid (DBSA) and the amphiphile p-(n-dodecyl)phenol (DP). We assume that the polar head of the amphiphile DP is somewhat similar to that of the resin.

Figure 13 plots the amount of the precipitated asphaltene vs. mole fraction of CO_2 for resin concentrations of 1.84 (content in original crude), 2.30, 2.76 and 3.68% (mol). The results reveal that an increase in the resin concentration inhibits the asphaltene precipitation. When the concentration of resin increases to 3.96%, there is no precipitation up to a CO_2 concentration of 65.3%. Experimental data by Espinat and Ravey (1993) have shown that the micellar size decreases with the increase of resin concentration in a crude. Figure 14 demonstrates that the predicted micellar core radius decreases with the increase of resin concentration, which is in agreement with the experimental data. Next, we use the model to predict the efficiency of DBSA in asphaltene precipitation inhibition.

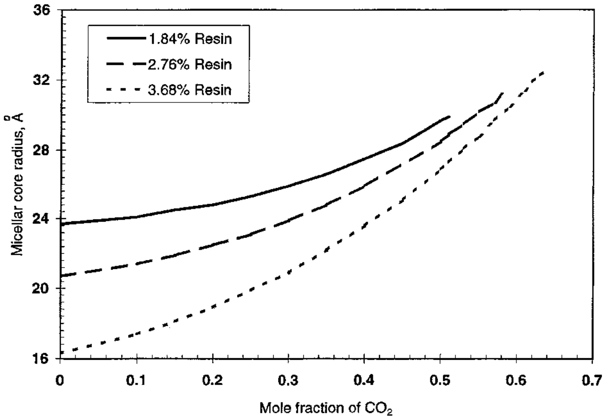

Figure 14. Effect of resin concentration on the micellar size.

Weyburn reservoir fluid and CO_2 mixture at 160 bar and 332 K.

The molar volume of DBSA is 316.5 cm^3/mol (Kosswig, 1994), but the critical properties (Tc and Pc) and the acentric factor (ω) are not available. However, the computed results are not sensitive to Tc, Pc, and ω (to be discussed later). Therefore, we use the same Tc, Pc, and ω values as for DP (to be given later). The structural parameters of the polar head for DBSA are $a_0 = 17$ Å^2 and $a_p = 17$ Å^2 (Nagarajan and Ruckenstein, 1991). A strong interaction between the polar head of DBSA and asphaltene species has been reported by Chang and Fogler (1994a,b). We assume the molar adsorption enthalpy of DBSA $(\Delta h_f^0)_{\text{Adp}}$ to be five times the enthalpy of formation of the hydrogen bond, -11.2×10^3 J/mol; $(\Delta h_f^0)_{\text{Adp}} = -56.0 \times 10^3$ J/mol. The model results are not sensitive to $(\Delta h_f^0)_{\text{Adp}}$ when its absolute value is large. Figure 15 shows the effect of DBSA concentration on precipitation. Compared with resin (see Figure 13), DBSA is much more effective. Some unique features of DBSA predicted from the model are:

- Almost all the DBSA molecules adsorb onto the micellar core surface. The ratio of the molecular number of DBSA in the micellar shell to that in the bulk phase is over 10^8.

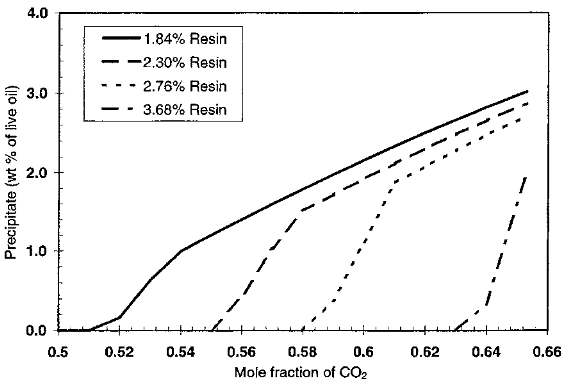

Figure 13. Effect of resin concentration (mol %) on asphaltene precipitation.

Weyburn reservoir fluid and CO_2 mixture at 160 bar and 332 K.

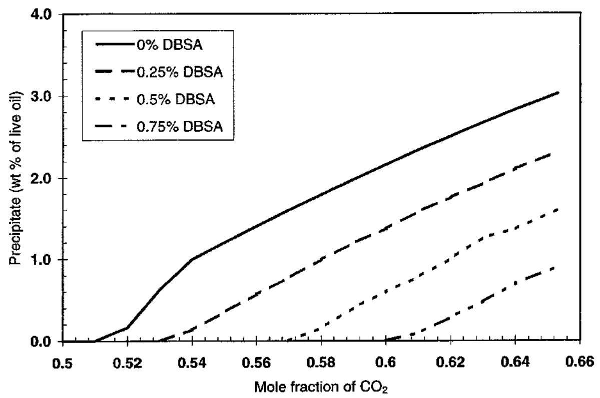

Figure 15. Effect of DBSA concentration (mol %) on asphaltene precipitation.

Weyburn reservoir fluid and CO_2 mixture at 160 bar and 332 K.

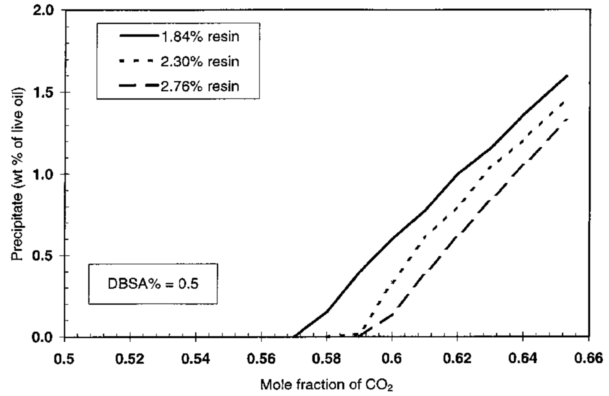

Figure 16. Effect of resin concentration (mol %) on asphaltene precipitation.

Weyburn reservoir fluid, CO_2 and DBSA mixture at 160 bar and 332 K.

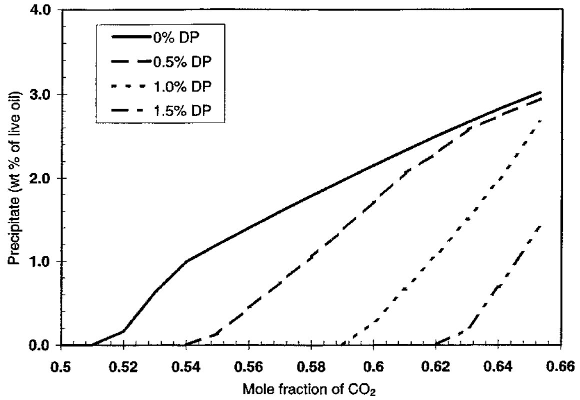

Figure 17. Effect of DP concentration (mol %) on asphaltene precipitation.

Weyburn reservoir fluid and CO_2 mixture at 160 bar and 332 K.

- The molecular number of asphaltene in the micellar core n_1 is constant; it is independent of the concentrations of DBSA, resin, and CO_2.
- The molecular number n_2 of resin, and n_f of DBSA in the shell are nearly independent of the concentrations of DBSA, resin and CO_2.
- Precipitation and micellar size are nearly independent of the structural parameters of the polar head a_0 and a_p of DBSA. We used $a_0 = 21.7$ Å^2 (1.25 times of the original), and $a_p = 21.7$ Å^2 (1.25 times of the original) and found the calculated results vary very little.
- The predicted results are also insensitive to v_f, Tc, Pc, and ω of DBSA. Increase of v_f to 474.7 from 316.5 cm^3/mol, Tc to 800 from 779 K, Pc to 20 from 18 bar, and ω to 1.20 from 1.08 have very little effect on precipitation.
- The effect of resin concentration on precipitation becomes less pronounced after DBSA is mixed with the crude. Figure 16 plots the effect of resin concentration on asphaltene precipitation with 0.5% DBSA in the crude (see Figures 13 and 16).

Table 2 provides the contribution of each term of Eq. 25 per molecule of asphaltene, resin, and DBSA; $(\Delta h_f^0)_{\mathrm{Adp}}$ is the dominant term, and it depends only on temperature. The large negative value of $(\Delta h_f^0)_{\mathrm{Adp}}$ is the main reason that nearly all DBSA molecules move to the shell reducing the Gibbs free energy of the total system. At low amphiphile concentration, almost all DBSA molecules adsorb onto the micellar core surface together with the co-adsorption of some resins. A certain amount of resin can saturate the micellar surface; beyond that, an increase of resin amount does not result in micellar stability, as the results show in Figure 16.

The thermodynamic properties of DP are obtained by extrapolating the data of the alkylphenols of different chain lengths from Daubert and Danner (1988); $Tc = 779$ K, $Pc = 18.0$ bar, $\omega = 1.08$, and $v_f = 281.0$ cm^3/mol. The structural parameters of the polar head are $a_0 = 21$ Å^2 and $a_p = 40$ Å^2 (Nagarajan and Ruckenstein, 1991). The interaction between a DP molecule and an asphaltene molecule is weaker than that between DBSA and asphaltene (Chang and Fogler, 1994a,b). We set the adsorption enthalpy $(\Delta h_f^0)_{\mathrm{Adp}}$ of DP to twice that of the enthalpy of the formation of the hydrogen bond; $(\Delta h_f^0)_{\mathrm{Adp}} = -22.4 \times 10^3$ J/mol. Figure 17 shows the amount of precipitated asphaltene vs. CO_2 mole fraction for different DP concentrations. The effectiveness of DP is less than that of DBSA. The sensitivity to the structural parameters and thermodynamic properties is also examined. The increase of a_0 to 25 from 21 Å^2, a_p to 44 from 40 Å^2, v_f to 337 (1.2 times) from 281.0 cm^3/mol, and $(\Delta h_f^0)_{\mathrm{Adp}}$ to -26.9×10^3 J/mol from -22.4×10^3 J/mol moves the onset from 0.54 to 0. 55, 0.54 to 0.53, 0.54 to 0.55, and 0.54 to 0.56, respectively. The increase in Tc, Pc, and ω for 10 K, 2 bar, and 0.2, respectively, has very little effect on the precipitation. The computed results show that about 75% of total DP molecules are in the micellar shell. Table 3 lists the contribution of various terms to ΔG_m^{00}. No single term dominates ΔG_m^{00}. Increasing a_0 of the amphiphile decreases the interfacial energy term

Table 2. Contribution of Various Terms to ΔG_m^{00} (Unit, kT) for Mixture of the Weyburn Oil with 60 mol % CO_2 and 0.5% DBSA

Asphaltene:
$(\Delta g_a^0)_{\mathrm{Ass}} = -6.5$; $(\Delta g_a^0)_{\mathrm{Tr}} = -6.8$; $(\Delta g_a^0)_{\mathrm{Def}} = 0.6$
Resin:
$(\Delta g_r^0)_{\mathrm{Ste}} = 2.6$; $(\Delta h_r^0)_{\mathrm{Adp}} = -4.1$; $(\Delta g_r^0)_{\mathrm{Inf}} = 4.6$;
$(\Delta g_r^0)_{\mathrm{Tr}} = -4.9$; $(\Delta g_r^0)_{\mathrm{Def}} = 0.07$
DBSA:
$(\Delta g_f^0)_{\mathrm{Ste}} = 0.5$; $(\Delta h_f^0)_{\mathrm{Adp}} = -20.3$; $(\Delta g_f^0)_{\mathrm{Inf}} = 5.4$;
$(\Delta g_f^0)_{\mathrm{Tr}} = -2.7$; $(\Delta g_f^0)_{\mathrm{Def}} = 0.74$

Table 3. Contribution of Various Terms to ΔG_m^{00} (Unit, kT) for Mixture of the Weyburn Oil with 56 mol % CO_2 and 0.5% DP

Asphaltene:
$(\Delta g_a^0)_{\mathrm{Ass}} = -6.5$; $(\Delta g_a^0)_{\mathrm{Tr}} = -6.5$; $(\Delta g_a^0)_{\mathrm{Def}} = 0.6$
Resin:
$(\Delta g_r^0)_{\mathrm{Ste}} = 2.0$; $(\Delta h_r^0)_{\mathrm{Adp}} = -4.1$; $(\Delta g_r^0)_{\mathrm{Inf}} = 4.8$;
$(\Delta g_r^0)_{\mathrm{Tr}} = -4.7$; $(\Delta g_r^0)_{\mathrm{Def}} = 0.02$
DP:
$(\Delta g_f^0)_{\mathrm{Ste}} = 2.0$; $(\Delta h_f^0)_{\mathrm{Adp}} = -8.1$; $(\Delta g_f^0)_{\mathrm{Inf}} = 4.8$;
$(\Delta g_f^0)_{\mathrm{Tr}} = -2.5$; $(\Delta g_f^0)_{\mathrm{Def}} = 0.64$

$(\Delta g_f^0)_{\rm Inf}$ (see Eq. 19b), which favors the micellar stability. However, increasing a_p increases $(\Delta g_f^0)_{\rm Ste}$ (see Eq. 23b), which opposes the micellar stability.

Discussion

An aromatic solvent can stabilize the asphaltene micelles through a decrease of the interfacial tension between the asphaltene core and the shell. The predicted results from the model show consistently that the concentration of the aromatic solvent in the shell can be several times more than in the bulk. The key parameter in asphaltene precipitation inhibition by aromatic solvents is the interfacial tension σ. Experimental data is mainly limited to simple systems. Quantitative data for crude/aromatic solvents will be valuable in model verification. Such quantitative data currently do not exist.

Resin molecules may not self-associate in the crude, mainly because of the weak polar head. The polarity of the head of the resin molecule is about the same as the phenol group with or without other hydrocarbon groups between the benzene ring and the OH group. The interaction between resin and asphaltene is due to the H^+ in the OH group, similar to DP. The computations for the resin, DBSA, and DP show that the adsorption enthalpy is by far the most important parameter for an amphiphile. Since the adsorption enthalpy of resin is likely to be less than that of DBSA, resin may not be the most suitable chemical for efficient inhibition of asphaltene precipitation. The results from our model demonstrate that a main criterion for the selection of an amphiphile is the adsorption enthalpy, which may be obtained through measuring the heat of adsorption of an amphiphile in the liquid asphaltene. An effective amphiphile usually has a strong polar head. It may self-associate in the crude at high concentrations, as does DBSA in heptane (Chang and Fogler, 1994a).

Conclusions

The proposed thermodynamic micellization model can predict all the features of asphaltene precipitation inhibition in the crude. The model predicts a much higher concentration of the aromatic solvent in the shell than in the bulk phase. The higher concentration of an aromatic solvent in the shell decreases the interfacial tension between the asphaltene micellar core and the shell. The decrease in the interfacial energy of micelle stabilizes the micelle.

The interaction between an asphaltene and an amphiphile molecule is the most important parameter for the stabilization of the asphaltene micelles in crude. The strong interaction is drawn from the adsorption enthalpy of the amphiphile onto the micellar surface. The adsorption enthalpy can be used as the most important criterion to search for an efficient amphiphile. Resin may not be the most effective chemical for the inhibition, because the interaction between resin and asphaltene is not as strong as that of amphiphiles (such as alkylsulfonic acid or alkylbenzenesulfonic acid). For an amphiphile which has a strong interaction with the asphaltene, the adsorption energy dominates the micellar formation; other parameters may have little effect on the micellar stability. In some amphiphiles, both the adsorption enthalpy and the structure of the polar head contribute to the micellar stability. An effective amphiphile that has a strong polar head may self-associate and precipitate in the crude beyond a certain concentration. The model described in this article can be further extended to include the self-association of amphiphile molecules in order to predict the optimal concentration of an amphiphile for inhibition. The model may also be extended to include the effect of the tail length of the amphiphiles on asphaltene precipitation.

Acknowledgment

This work was supported by the members of the Reservoir Engineering Research Institute. Their support is greatly appreciated. We are also indebted to Prof. A. L. Tits, Electrical Engineering Department, University of Maryland for providing the code of the FSQP algorithm.

Notation

$a_{0,f}$ = cross-sectional area of the polar head of an amphiphile molecule
$a_{0,r}$ = cross-sectional area of the polar head of a resin molecule
$a_{p,f}$ = effective cross-sectional area of an amphiphile molecule attached to the polar head
$a_{p,r}$ = effective cross-sectional area of a resin molecule attached to the polar head
c = critical property
f = fugacity
k = Boltzmann constant
m = ratio of asphaltene, resin or amphiphile to solvent molecular volume
M = molecular weight
n = molecular number
N = molecular number
P = pressure
T = temperature
x = molecular fraction
$(\Delta G^0)_{\rm Inf}$ = interfacial free energy of a micelle
$(\Delta G^0)_{\rm Str}$ = steric repulsion free energy of a micelle
$(\Delta g_a^0)_{\rm Def}$ = deformation free energy of an asphaltene molecule in the micellar core
$(\Delta G_a^0)_{\rm Def}$ = deformation free energy of n_1 asphaltene molecules in the micellar core
$(\Delta g_a^0)_{\rm Ass}$ = association free energy of an asphaltene molecule in the micellar core
$(\Delta G_a^0)_{\rm Ass}$ = association free energy of n_1 asphaltene molecules in the micellar core
$(\Delta g_a^0)_{\rm Tr}$ = transfer free energy of an asphaltene molecule from an infinite dilute solvent medium in bulk to a micelle
$(\Delta G_a^0)_{\rm Tr}$ = transfer free energy of n_1 asphaltene molecules from an infinite dilute solvent medium in bulk to a micelle
$(\Delta G_r^0)_{\rm Adp}$ = adsorption free energy of n_2 resin molecules on the surface of a micelle
$(\Delta g_r^0)_{\rm Def}$ = deformation free energy of a resin molecule in the micellar shell
$(\Delta G_r^0)_{\rm Def}$ = deformation free energy of n_2 resin molecules in the micellar shell
$(\Delta g_r^0)_{\rm Inf}$ = portion of the interfacial free energy based on a resin molecule
$(\Delta G_r^0)_{\rm Inf}$ = portion of the interfacial free energy based on n_2 resin molecules
$(\Delta g_r^0)_{\rm Tr}$ = transfer free energy of a resin molecule from an infinite dilute solvent medium in bulk to the shell
$(\Delta G_r^0)_{\rm Tr}$ = transfer free energy of n_2 resin molecules from an infinite dilute solvent medium in bulk to the shell
$(\Delta G_f^0)_{\rm Adp}$ = adsorption free energy of n_f amphiphile molecules on the surface of a micelle
$(\Delta g_f^0)_{\rm Def}$ = deformation free energy of an amphiphile molecule in the micellar shell
$(\Delta G_f^0)_{\rm Def}$ = deformation free energy of n_f amphiphile molecules in the micellar shell

$(\Delta g_f^0)_{\text{Inf}}$ = portion of the interfacial free energy based on an amphiphile molecule
$(\Delta G_f^0)_{\text{Inf}}$ = portion of the interfacial free energy based on n_f amphiphile molecules
$(\Delta g_f^0)_{\text{Str}}$ = steric repulsion free energy of an amphiphile molecule in the micellar shell
$(\Delta G_f^0)_{\text{Str}}$ = steric repulsion free energy of n_2 amphiphile molecules in the micellar shell
$(\Delta g_r^0)_{\text{Str}}$ = steric repulsion free energy of a resin molecule in the micellar shell
$(\Delta G_r^0)_{\text{Str}}$ = steric repulsion free energy of n_2 resin molecules in the micellar shell
$(\Delta g_f^0)_{\text{Tr}}$ = transfer free energy of an amphiphile molecule from an infinite dilute solvent medium in bulk to the shell
$(\Delta G_f^0)_{\text{Tr}}$ = transfer free energy of n_f amphiphile molecules from an infinite dilute solvent medium in bulk to the shell
$(\Delta h_f^0)_{\text{Adp}}$ = adsorption enthalpy of an amphiphile molecule on the surface of the micellar core
$(\Delta h_r^0)_{\text{Adp}}$ = adsorption enthalpy of a resin molecule on the surface of the micellar core

Superscripts

l = pure liquid phase state of a species
$*$ = standard state at infinite dilution
∞ = infinite dilution

Subscripts

a = asphaltene
a_1 = monomeric asphaltene
f_1 = monomeric amphiphile
0 = standard state at 298 K and 1 bar

Literature Cited

Andersen, S. I., and J. G. Speight, "Observations on the Critical Micelle Concentration of Asphaltenes," *Fuel*, **72**, 1343 (1993).

Chang, C.-L., and H. S. Fogler, "Stabilization of Asphaltenes in Aliphatic Solvents Using Alkylbenzene-Derived Amphiphiles: 1. Effect of the Chemical Structure of Amphiphiles on Asphaltene Stabilization," *Langmuir*, **10**, 1749 (1994a).

Chang, C.-L., and H. S. Fogler, "Stabilization of Asphaltenes in Aliphatic Solvents Using Alkylbenzene-Derived Amphiphiles: 2. Study of the Asphaltene-Amphiphile Interactions and Structures Using Fourier Transform Infrared Spectroscopy and Small-Angle X-Ray Scattering Techniques," *Langmuir*, **10**, 1758 (1994b).

Cimino, R., S. Correra, A. D. Bianco, and T. P. Lockhat, "Solubility and Phase Behavior of Asphaltenes in Hydrocarbon Media," *Asphaltenes: Fundamentals and Applications*, Chap. 3, E. Y. Sheu and O. C. Mullins, eds., Plenum Press, New York (1995).

Daubert, T. E., and R. P. Danner, *Physical and Thermodynamic Properties of Pure Chemicals: Design Institute for Physical Property Data*, Hemisphere Publishing Corp., New York (1988).

De Boer, R. B., K. Leerlooyer, M. R. P. Eigner, and A. R. D. Van Bergen, "Screening of Crude Oils for Asphalt Precipitation: Theory, Practice, and the Selection of Inhibitors," *SPE Production & Facilities*, 55 (Feb. 1995).

Espinat, D., and J. C. Ravey, "Colloidal Structure of Asphaltene Solutions and Heavy-Oil Fractions Studied by Small Angle Neutron and X-Ray Scattering," paper SPE 25187, *Spe Int. Symp. on Oilfield Chemistry*, New Orleans (Mar. 2–5, 1993).

Firoozabadi, A., *Thermodynamics of Hydrocarbon Reservoirs*, Chap. 5, McGraw-Hill, New York (1999).

Gonzalez, G., and A. Middea, "Peptization of Asphaltene by Various Oil Soluble Amphiphiles," *Colloids and Surfaces*, **42**, 207 (1991).

Hirschberg, A., L. N. J. de Jong, B. A. Schipper, and J. G. Meijers, "Influence of Temperature and Pressure on Asphaltene Flocculation," *SPE J.*, 283 (June, 1984).

Iyer, S., Private Communication, Shell Oil Company, Houston (Nov. 1998).

Kosswig, K., "Sulfonic Acids, Aliphatic," *Ullmann's Encyclopedia of Industrial Chemistry*, **A25**, 503 (1994).

Lian, H., J.-R. Lin, and T. F. Yen, "Peptization Studies of Asphaltene and Solubility Parameter Spectra," *Fuel*, **73**, 423 (1994).

Nagarajan, R., "Micellization, Mixed Micellization and Solubilization: The Role of Interfacial Interaction," *Adv. Colloid Interface Sci.*, **26**, 205 (1986).

Nagarajan, R., and E. Ruckenstein, "Theory of Surfactant Self-Assembly: A Predictive Molecular Thermodynamic Approach," *Langmuir*, **7**, 2934 (1991).

Pan, H., and A. Firoozabadi, "Thermodynamic Micellization Model for Asphaltene Aggregation and Precipitation in Petroleum Fluids," *SPE Production & Facilities*, 118 (May 1998).

Pan, H., and A. Firoozabadi, "Thermodynamic Micellization Model for Asphaltene Precipitation from Reservoir Crudes at High Pressures and Temperatures," *SPE Production & Facilities* (Feb. 2000).

Puvvada, S., and D. Blankschtein, "Theoretical and Experimental Investigations of Micellar Properties of Aqueous Solutions Containing Binary Mixtures of Nonionic Surfactants," *J. Phys. Chem.*, **96**, 5579 (1992).

Rogacheva, O. V., R. N. Rimaev, V. Z. Gubaidullin, and D. K. Khakimov, "Investigation of the Surface Activity of the Asphaltenes of Petroleum Residues," *Colloid J. USSR*, 490 (1980).

Sheu, E. Y., and D. A. Storm, "Colloidal Properties of Asphaltenes in Organic Solvents," *Asphaltenes: Fundamentals and Applications*, E. Y. Sheu and O. C. Mullins, eds., Chap. 1, Plenum Press (1995).

Sirvastava, R. K., S. S. Huang, S. B. Dyer, and F. M. Mourits, "Quantification of Asphaltene Flocculation During Miscible CO_2 Flooding in the Weyburn Reservoir," *J. Can. Pet. Tech.*, **34**, 31 (1995).

Speight, J. G., *The Chemistry and Technology of Petroleum*, Chap. 5, Marcel Dekker, New York (1980).

Storm, D. A., and E. Y. Sheu, "Characterization of the Asphaltenic Colloidal Particle in Heavy Oil," *Fuel*, **74**, 1140 (1995).

Wiehe, L. A., and K. S. Liang, "Asphaltenes, Resins, and Other Petroleum Macromolecules," *Fluid Phase Equil.*, **117**, 201 (1996).

Zhou, J. L., A. L. Tits, and C. T. Lawrence, "User's Guide for FFSQP Version 3.6: A FORTRAN Code for Solving Constrained Nonlinear (Minimax) Optimization Problems, Generating Iterates Satisfying All Inequality and Linear Constraints," Electrical Engineering Dept., Univ. of Maryland, College Park (1996).

Manuscript received Dec. 28, 1998, and revision received July 16, 1999.